

### 3 Underlying Technology

The underlying technology activity includes five tasks:

- Laser-induced removal of fuel and co-deposits from plasma facing components in tokamaks and characterisation of laser-irradiated surfaces
- Mathematical modelling of thermal-hydraulic problems in cable in conduit conductors
- FGM W-Cu composites and W-Cu /W joints fabrication route based on pulse plasma sintering (PPS) method
- Applications of hydrostatic extrusion for particles and grains size refinement in materials relevant to the fusion technologies
- Modelling and optimisation of thermo-mechanical behaviours of W-Cu and W-CuCrZr functionally graded composites (FGCs)

### 3.1 Laser-induced removal of fuel and co-deposits from plasma facing components in tokamaks and characterisation of laser-irradiated surfaces

*Jerzy Wołowski*

*Institute of Plasma Physics and Laser Microfusion*

*wolowski@ifpilm.waw.pl*

*P. Gąsior, A. Czarnecka, M. Kubkowska, P. Parys, M. Rosiński, J. Hoffman, Z. Szymański, V. Philipps, and M. Rubel*

#### Abstract

Laser induced ablative co-deposit removal is one among most convenient methods to be used in next-step fusion devices, especially when considering removal of layers present in the areas which aren't easily accessible for other methods (eg. castellated components and louvers). In recent years the method has been extensively investigated and developed at DLP IPPLM with the use of Nd-YAG repetitive laser system operating at 10 Hz with 3 ns, 0.6 J pulses at the wavelength of 1064 nm. The report contains the results obtained in 2007 which mainly consider optimisation of the removal process with scanning beam, investigation of dust generated by the laser ablation and estimating the best parameters for spectroscopic real time monitoring of the method.

#### Summary

The experiments with scanning beam at velocities up to 5 mm/s proved to be efficient method of laser ablation codeposit removal with the laser system present at IPPLM Warsaw. The spectrometry technique used for the process monitoring turned out to be a robust diagnostics method which can be also used for the controlling of the process in near future. The research performed in the collaborating laboratories proved that the laser treated surface was free from deuterium and that the co-deposited layer has been removed.

The investigation of the generation of dust allowed for characterization of the dust particles size, distribution and chemical composition. The distribution of diameter with near Gaussian shape and mean value in range of a fraction of  $\mu\text{m}$  suggested that the laser ablation process may be used as a sample dust generator for investigation of dusts present in tokamak vessels. SEM pictures of the collected dust showed that it has a structure of codeposit flakes and NRA measurements indicated still quite high deuterium amounts at level of  $3.9 \times 10^{17}$  particles per  $\text{cm}^2$ .

The investigation of optimal condition for spectrometric observation of laser ablation process confirmed that the spectroscopic signal has the best parameters while the irradiation point is shifted from the focus by  $\sim 10\%$  of focal length, but it was also proved that the signal could be observed in wide range of power density at the target.

#### Conclusions

All the milestones which were specified in the Work Programme for 2007 have been realized, in particular the following highlights may be listed:

- Development of the scanning beam stage with optimal irradiation condition
- Tests of scanning speeds in range of 1-10 mm/s
- Estimation of optimal conditions for spectroscopic measurements for carbon based materials and tungsten
- First results of dust investigation

The recent research on laser-induced removal of fuel and co-deposits from plasma facing components in tokamaks and characterisation of laser-irradiated surfaces carried on at IPPLM in 2007 allowed to realize its main purpose which was investigation of a scanning beam method for ablative laser removal. The process optimization was based on the measures of spectroscopic diagnostics which have been proved to be effective method for the process monitoring in real time.

Another long term purpose which was realized in 2007 was preliminary dust investigation which was good starting point for advanced research in near future.

The next step research on the topic should concern developing an automated stage for the co-deposited layers removal and further investigation of the dust with the use of real-time and post-mortem diagnostics.

#### Collaboration

Association EURATOM – FZJ, Institute of Plasma Physics, Juelich, Germany

Association EURATOM – VR, Royal Institute of Technology, Stockholm, Sweden.

#### References

- [1] P. Gašior and J. Wołowski, Report “Deliverable D4” “*Possible measurements of dust produced during plasma transients*”, EFDA Rep. TW6-TSS-SEA 5.1, 2007
- [2] P. Gašior, J. Compan, A. Czarnecka, B. Emmoth, T. Hirai, J. Linke, B. Kolman, P. Parys, M. Rosiński, M. Rubel, P. Sundelin, E. Wessel, J. Wołowski, “*Microstructures of co-deposited layer on plasma-facing carbon surfaces after high power laser treatments*”, contribution to EUROMAT 2007, 10 - 13 September, Nuremberg, Germany
- [3] P. Gašior, B. Emmoth, T. Hirai, F. Irrek, J. Linke, B. Kolman, V. Philipps, P. Sundelin, M. Rubel, E. Wessel, J. Wołowski, “*Laser induced removal of co-deposits from graphitic plasma facing components*”, 34th EPS Conference on Plasma Physics, 2-6 July 2007, Warsaw, Poland
- [4] P. Gašior, J. Wołowski, A. Czarnecka, M. Rosiński, “*Dust diagnostics in the next-step fusion devices – study performed at IPPLM*”, Workshop: “Association Days”, Kudowa, Poland, 18-20, Sept. 2007

### 3.2 Mathematical modeling of thermal – hydraulic problems in Cable-in-Conduit Conductors (CICCs)

*Monika Lewandowska*  
*Szczecin University of Technology*  
*monika.lewandowska@ps.pl*

*Monika Lewandowska, Leszek Malinowski, and Wojciech Rachtan*

#### Abstract

Recently the reduction of the void fraction in the bundle region of the TF coil CICC, to the range of 0.28-0.30, has been decided in the ITER magnet community to improve the conductor performance under electromagnetic forces. Hence, the impact of a low void fraction on the CICCs' hydraulic properties must be reliably assessed. The experimental investigation of the bundle friction factor as a function of Reynolds number on single channel CICCs with different void fraction and various cabling patterns has been performed at the EPFL-CRPP (Villigen PSI). The experimental results have been compared with the Katheder correlation and analyzed using the porous medium model of the CICC's bundle. Porous medium model has confirmed its applicability as an important tool for CICC cable bundle flow analysis. A review of published experimental data for the bundle friction factor and existing relevant correlations is also presented.

#### Summary

The following tasks has been realized in 2007 year

1. An extensive literature survey has been performed and the database of bibliography related to thermal-hydraulic problems in superconducting cables and in porous media has been created.
2. A database of the friction factor experimental data and existing correlations has been established. It has been observed that most of the existing correlations for friction factors in CICCs were obtained by ad hoc modifications of the known correlations for pipe flow and by fitting to experimental data measured for individual conductors, i.e. they are not based on any established theory.
3. Collaborative processing and analysis of the data arising from two experimental campaigns devoted to the investigation of bundle friction factor coefficients in CICCs as a function of the void fraction have been completed. A number of pressure drop measurements have been performed by our partners at the EPFL-CRPP (Villigen PSI) using single channel subsize CICCs with different cabling patterns. The cables have been compacted three times to reduce the void fraction in the range of 0.25-0.35. The longitudinal bundle friction factor has been deduced from measurements of pressure drop and mass flow rate at each stage of compaction. The experimental results have been compared with correlations proposed by Katheder and others resulting from the porous medium analogy model. A dependence of the bundle friction factor on the cabling pattern has been observed (see Fig.1). It seems that an additional parameter related to the cabling pattern should be taken into account while formulating of a new correlation for the bundle friction factor.
4. Porous medium model has confirmed its applicability as an important tool for CICC cable bundle flow analysis. It predicts the linear dependence of the friction factor on  $1/Re$  for any CICC bundle configuration:

$$f_{Eu} = \frac{2D_h^2 \phi}{K} \frac{1}{Re} + \frac{2D_h \phi^2 C_F}{\sqrt{K}}$$

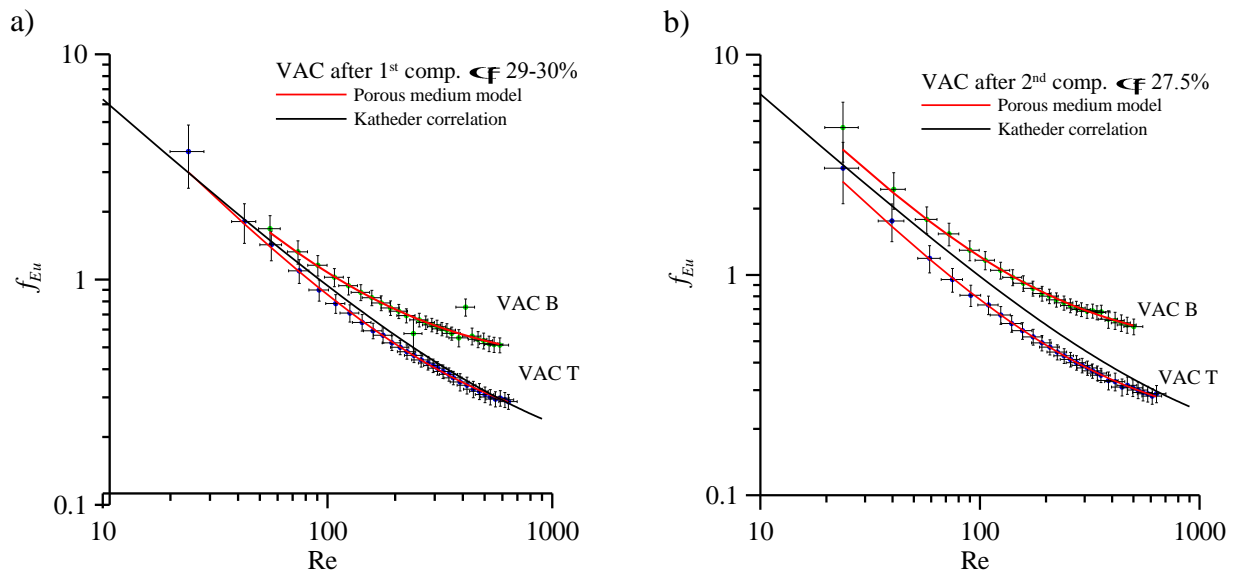


**Figure 1** Friction factor as a function of the Reynolds number for VAC B and VAC T samples after the first (a) and second (b) compaction. The best-fitting porous medium model and the Katheder correlations are also shown.

This correlation agrees well with the available experimental data (see Fig. 1). The values of the porous medium parameters, i.e. permeability  $K$  and drag coefficient  $C_F$ , can be computed for each individual CICC by fitting to experimental data, but predictive use of the above equation would require an a priori determination of them. It is known that  $K$  and  $C_F$  may depend on the porosity (void fraction) and on the geometrical parameters of the medium (cabling pattern), but the way of computing them for CICC bundle is not yet established. Research efforts aimed at the formulation of a new correlations for the  $K$  and  $C_F$  are in progress.

5. Acquaintance with the FLUENT software for thermo-hydraulic calculations has been made and modeling of a CICC has been started with the aid of the FLUENT.
  - A search for literature dealing with the application of the software package “FLUENT” to modelling fluid flow and heat transfer in channels has been conducted. Analysis of the literature has been performed.
  - The „FLUENT” software has been put into operation. A number of sample problems have been solved.

## Conclusions

- The existing correlations for the friction factors in CICC are not quite satisfactory and they are not based on any established theory.
- A dependence of the bundle friction factor on the cabling pattern has been observed experimentally. We suggest that an additional parameter related to the cabling pattern should be introduced while formulating of a new correlation for the bundle friction factor.
- Porous medium model has confirmed its applicability as an important tool for CICC cable bundle flow analysis. The research directed to the establishment of a new predictive correlation for the bundle friction factor, based on the porous medium model is in progress and should be completed in the following year.

## Collaboration

Association EURATOM – Swiss Confederation, EPFL-CRPP, Villigen PSI, Switzerland  
CERN, AT Department, Geneva, Switzerland

**List of symbols**

$C_F$  - drag coefficient of the porous medium, -  
 $D_h$  - hydraulic diameter, m  
 $f$  - friction factor, -  
 $K$  - permeability of the porous medium, m<sup>2</sup>  
 $Re$  - Reynolds number,  
 Greek  
 $\varphi$  - void fraction (porosity), -

**References**

- [1] Minutes of ITER meetings on conductor “crash action” on October 3<sup>rd</sup> and November 15<sup>th</sup> 2006
- [2] P. Bruzzone, B. Stepanov, R. Wesche, IEEE Trans. Appl. Supercon. 13, pp. 1452-1455 (2003)
- [3] P. Bruzzone, B. Stepanov, R. Wesche, Adv. Cryo. Eng. 52, pp. 558-565 (2006)
- [4] Van Sciver, Helium cryogenic. New York. Plenum Press (1986)
- [5] Vandoni G., Heat transfer. CERN Accelerator school, 8-17 May 2002, CERN
- [6] F. M. White, Fluid Mechanics, McGraw-Hill, New York 1994
- [7] S. L. Qi, P. Zhang, R. Z. Wang, L. X. Xu, Int. J. Heat Mass Trans. 50, pp. 1993-2001 (2007)
- [8] K. Hamada, Y. Takahashi, N. Koizumi, H. Tsuji, A. Anghel, B. Blau, A. Fuchs, B. Heer, G. Vecsey, S. Smith, S. Pourrahimi, M. Zhemlamskij, Adv. Cryo. Eng. 43 (A), pp. 197-204 (1998)
- [9] P. Bruzzone, Pressure Drop and Helium Inlet in ITER CS1 Conductor, 21st SOFT Conference (2000)
- [10] S. Nicollet, J.-L. Duchateau, H. Fillunger, A. Martinez, S. Parodi, IEEE Trans. Appl. Supercon. 10, pp. 1102-1105 (2000)
- [11] S. Nicollet, D. Bessette, H. Cloez, P. Decool, B. Lacroix, C. A. Lebailly, J. P. Serries, Review of singular cooling inlet and linear pressure drop for ITER coils cable in conduit conductor, CEC-ICMC Conference, Colorado (2005)
- [12] S. Nicollet, H. Cloez, J.-L. Duchateau, J. P. Serries, Hydraulics of the ITER Toroidal Field model coil cable-in-conduit conductors, Proceedings of the 20th SOFT, pp. 771-774 (1998)
- [13] R. Zanino, P. Santagati, L. Savoldi, IEEE Trans. Appl. Supercon. 10, pp. 1066-1069 (2000)
- [14] M. Yamaguchi, T. Hamajima, H. Okuma, H. Ichikawa, A. Miura, Y. Sawada, Development of a 12T forced-cooled Toroidal Field coil, 10th ICEC, Helsinki (1984)
- [15] Y. Takahashi, E. Tada, K. Okuno, H. Tsuji, T. Ando, T. Hiyama, K. Koizumi, M. Nishi, H. Nakajima, K. Yoshida, T. Kato, K. Kawano, M. Oshikiri, Y. Hattori, R. Takahashi, S. Kamiya, S. Shimamoto, Experimental results of JF-15 forced-cooled superconducting test loop, 10th ICEC (1984)
- [16] S. Shimamoto, T. Ando, T. Hiyama, H. Tsuji, Y. Takahashi, M. Nishi, E. Tada, K. Yoshida, K. Okuno, K. Koizumi, H. Nakajima, T. Kato, K. Kawano, Y. Hattori, S. Kamiya, Y. Ohgane, E. Yaguchi, M. Oshikiri, Development of a large forced-flow cooled pulsed coil for the next tokamak, Proceedings of the IEEE 11th Symposium on Fusion Engineering, pp. 1017-1020 (1985)
- [17] T. Kato, E. Tada, Y. Takahashi, K. Okuno, H. Tsuji, T. Ando, T. Hiyama, K. Koizumi, H. Nakajima, O. Takahashi, K. Kawano, M. Oshikiri, M. Nishi, Y. Yoshida, Y. Hattori, R. Takahashi, S. Kamiya, S. Shimamoto, IEEE Trans. Mag. MAG-21, pp. 1095-1098 (1985)
- [18] X. Cheng, W. Lehmann, Cryogenics 34, pp. 607-610 [ICEC supplement] (1994)
- [19] M. Sugimoto, T. Kato, K. Kawano, T. Hiyama, Y. Kamiyachi, H. Ishida, S. Iwamoto, A. Miyake, H. Ebisu, K. Okuno, N. Koizumi, E. Tada, M. Nishi, H. Tsuji, M. Ono, H. Mukai, Y. Wachi, Cryogenics 33, pp. 597-602 (1993)
- [20] H. Katheder, NET Report N/R/0821/26/A (1992)
- [21] H. Katheder, Cryogenics 34, pp. 595-598 [ICEC supplement] (1994)
- [22] S. Nicollet, J.-L. Duchateau, H. Fillunger, A. Martinez, Cryogenic 40, pp. 569-575 (2000)
- [23] ITER Design Description Document. Magnet. Section 1: Engineering description, N 11 DDD 178 04-06-04 R 0.4 (2004)

### 3.3 FGM W-Cu composites and W-Cu /W joints fabrication route based on pulse plasma sintering (PPS) method

*Elżbieta Fortuna*

*Warsaw University of Technology, Materials Science and Engineering Faculty  
elaf@inmat.pw.edu.pl*

*Elżbieta Fortuna, Marcin Rosiński, Andrzej Michalski, Wojciech Lisowski,  
and Krzysztof J. Kurzydłowski*

#### Abstract

W-Cu composites and W-Cu/W joints were produced by pulse plasma sintering method (with constant and functionally graded composition). The microstructure of composites and joints were investigated and the physical properties determined.

#### Summary

##### 1. Development of W-Cu/W joining technology by PPS method

The W-Cu/W joints were produced using a PPS apparatus, constructed at the Faculty of Materials Science and Engineering, Warsaw University of Technology. Utilizing the experience gained in the fabrication of the composites with a constant W/Cu ratio as well as layered composites the conditions for joints production were established. The process parameters are given in Table 1.

**Table 1.** Process parameters in sintering of the W-Cu/W joints

Process parameters	Stage I	Stage II
Temperature [°C]	150	930
Duration of the individual process stages [s]	180	600
Charging voltage of the capacitors [kV]	2	5
Pulse repetition frequency [Hz]	1	1
Pressure [Pa]	$5 \cdot 10^{-3}$	$5 \cdot 10^{-3}$

Four types of joints were successfully produced by PPS method. The tungsten plates (1 mm thick, 12 mm diameter) were sintered with a composite material of different W/Cu proportions (25, 40, 50 and 60 vol.%). After sintering, joints were 3 mm high. The SEM examinations of the cross-sections of the joints revealed good bonding between the composites and tungsten plates, free of pores, cracks and delaminations (Fig. 1). The composite materials were fully sintered.

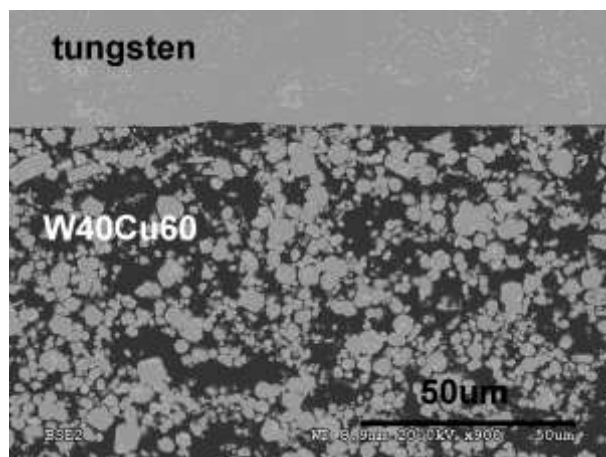


**Figure 1** SEM image of tungsten/W40Cu60 interface

2. Optimization of technology

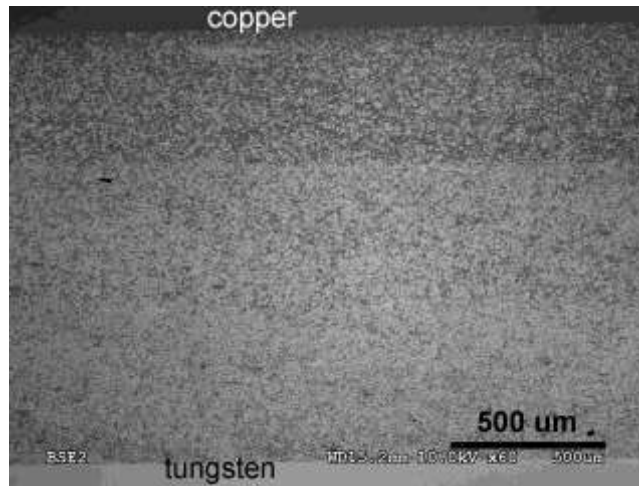


**Figure 2** SEM image of W/ sandwich-type composite/Cu joint

The technology for sandwich gradient materials was developed in 2006 (see 2006 Annual Report of Association EURATOM – IPLM). In 2007 the additional experiments were carried out in order to optimize the process and eliminate singular delaminations at the W40Cu60/W25Cu75 interface. The tungsten plate/layered composites with three different tungsten content (50, 40 and 25 vol.%) joints were sintered using process parameter given in Tab. 1. The plate was cylindrical in shape and had a diameter of 12 mm; the thickness of the individual layers was 0.5 mm. SEM examinations revealed good connections between sub-layers and plates and composite material. The composite material was free of pores and delaminations. The thickness reduction of the particular interlayers (from 1.5 to 0.5 mm) resulted in sandwich-type W/Cu composites with a good bonding between interlayers (Fig. 2).

3. Physical properties of the composites

Composites containing 25, 40 and 50 volumetric percent of tungsten were subjected to measurements of the coefficients of thermal conductivity. The results are presented in Fig. 3.

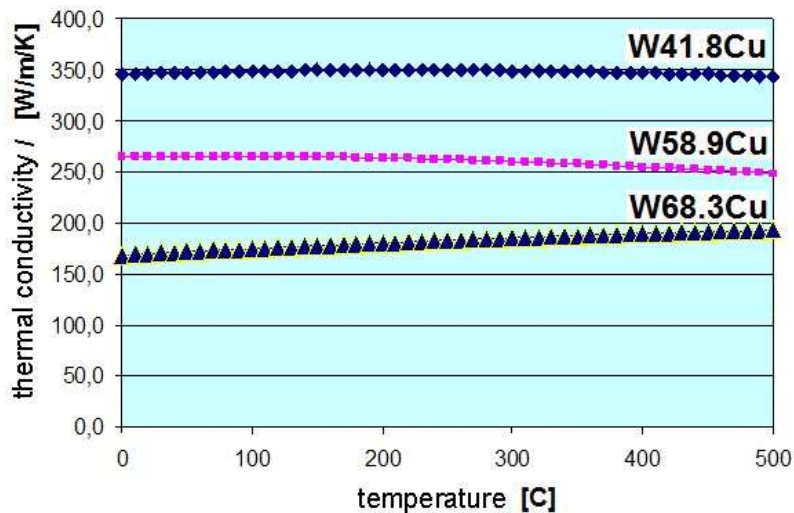


**Figure 3** Thermal conductivity of composites containing 25, 40 and 50 vol.% of tungsten (41.8, 58.9 and 68.3 wt. %)



### 3.4 Applications of hydrostatic extrusion for particles and grains size refinement in materials relevant to the fusion technologies

*Małgorzata Lewandowska*

*Warsaw University of Technology Faculty of Materials Science and Engineering  
malew@inmat.pw.edu.pl*

*Agnieszka Krawczyńska, Marcin Rasiński, and Krzysztof J. Kurzydłowski*

#### Abstract

The aim of the present work was to determine the possibility of the grain size reduction in Eurofer 97 to improve its mechanical properties via processing by hydrostatic extrusion (HE). Samples were hydrostatically extruded in a multi-step process with the total true strain of about 4. The results show that the HE leads to a significant grain refinement from about 400 nm to 86 nm at the same time particle size decreased from 111 nm to 75 nm and their distribution became more uniform. The mechanical behaviour (in tensile tests) of hydrostatically extruded Eurofer 97 steel over the wide range of temperatures (from -196°C to 600°C) was compared to those of the as-received material. It is clearly visible that the ultimate tensile strength and the yield stress are higher in the active range of temperatures for HE-processed samples. The results of microhardness measurements of the samples annealed at various temperatures have shown that the highest value of microhardness is achieved for samples annealed at 400°C - 403 HV0.2. The same applies to tensile and yield strength – their values start to decrease after the annealing at 600°C. At the same time elongation increases from 3 to 15%. It was revealed that post-extrusion annealing at 600°C substantially improves the strength-ductility balance in Eurofer 97 steel. Upon heating the initial grain size remains virtually unchanged up to a temperature of 600°C. However, at 800°C the grain size increases and will probably undergo intensive growth at higher temperatures.

#### Summary

Reduced activation ferritic-martensitic steel Eurofer 97 is a candidate material for structural applications in ITER reactor. The properties of such a steel strongly depend on its microstructure. This, in particular, applies to the grain size which influences such properties as hardness, flow stress, toughness and creep resistance. The aim of the present work was to determine the possibility of grain size reduction in Eurofer 97 to improve its mechanical properties via processing by hydrostatic extrusion (HE).

In this project, samples were hydrostatically extruded in a multi-step process with the total true strain of about 4. Microstructural changes induced by HE processing were observed using a light microscope, scanning and transmission electron microscopes. The mechanical properties were determined using an INSTRON 1115 testing machine at a strain rate of  $4 \times 10^{-4} \text{ s}^{-1}$  and Charpy impact test machine. In addition, microhardness was measured under the load of 200 g.

The results show that the HE leads to a significant grain refinement from about 400 nm to 86 nm (Table 1) at the same time particle size decreased from 111 nm to 75 nm and their distribution became more uniform.

**Table 1** Stereological parameters of grains in HE processed Eurofer 97 steel

State of Eurofer 97 steel	E(d <sub>2</sub> ) [nm]	SD(d <sub>2</sub> ) [nm]	CV(d <sub>2</sub> )	E(d <sub>max</sub> /d <sub>2</sub> )
As-received	400	206	0.52	1.56
HE-processed	86	31	0.36	1.59

E – mean value  
SD – standard deviation  
CV – coefficient of variation

The mechanical strength of hydrostatically extruded Eurofer 97 steel is higher over the wide range of test temperatures (from -196°C to 600°C) when compared to those of as-received state. However, the

ductility of HE processed materials is substantially lower. In order to determine thermal stability of HE-processed Eurofer 97 steel, the sample were annealed at various temperatures. The results of microhardness measurements have shown that the highest value of microhardness is achieved for samples annealed at 400°C - 403 HV0.2 whereas the lowest for samples annealed at 700°C - 228 HV0.2. The same applies to tensile and yield strength – their values start to decrease after the annealing at 600°C (Fig. 1). At the same time elongation increases from 3 to 15%. It was also revealed that upon heating the initial grain size remains virtually unchanged up to a temperature of 600°C. It is worth noting that post-extrusion annealing at 600°C substantially improves the strength-ductility balance in Eurofer 97 steel.

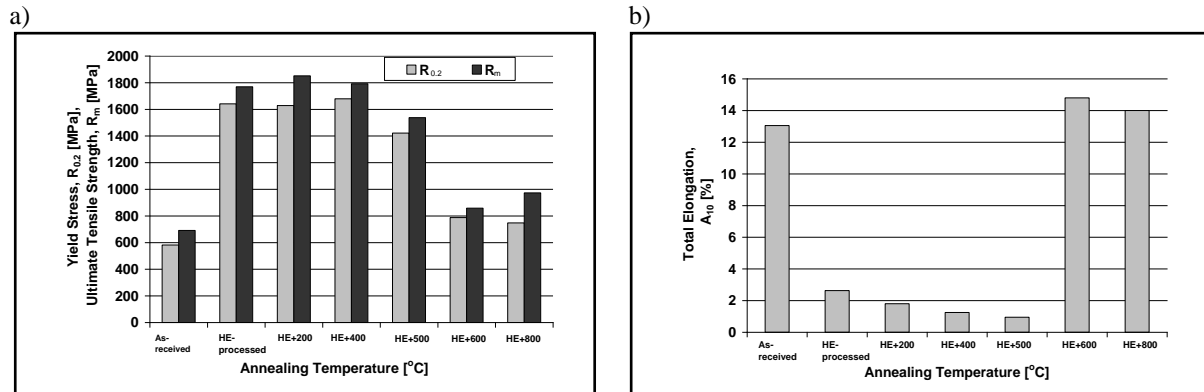


**Figure 1** Ultimate Tensile Stress  $R_m$  Yield Stress  $R_{0.2}$  (a), Total Elongation  $A_{10}$  (b)

## Conclusions

The results obtained in the present work clearly show that Eurofer 97 steel can be processed by HE to improve mechanical properties like the yield stress and the ultimate tensile strength. Such changes in mechanical properties are due to grain refinement down to nanometer scale which is stable to about 600°C. The improvement of the balance between mechanical strength and ductility of HE processed materials can be achieved by post-deformation annealing.

## References

- [1] M. Lewandowska, H. Garbacz, W. Pachla, A. Mazur, K. J. Kurzydłowski: Materials Science - Poland 23 (2005) 279-286
- [2] M. Lewandowska: Solid State Phenomena 114 (2006) 109-116
- [3] M. Lewandowska: Journal of Microscopy 224 (2006) 34-37
- [4] M. Lewandowska, K. J. Kurzydłowski: Materials Characterization 55 (2005) 395-401
- [5] H. Garbacz, M. Lewandowska, W. Pachla, K. J. Kurzydłowski: Journal of Microscopy 223 (2006)
- [6] M. Lewandowska, H. Garbacz, W. Pachla, A. Mazur, K. J. Kurzydłowski: Solid State Phenomena, 101 (2005) 65-69
- [7] FZKA 6911 report, Forschungszentrum Karlsruhe 2003

### 3.5 Modelling of thermo-mechanical behaviours of W-CuCrZr functionally graded composites (FGCs) as a technological aspect of structure optimisation

Lukasz Ciupiński

Materials Science and Engineering Faculty Warsaw University of Technology

lukas@inmat.pw.edu.pl

#### Abstract

The CuCrZr alloy is commonly used in the fusion as heat sink material. The W-CuCrZr graded composite interlayer can minimize the interface stresses of high heat flux components. The aim of this project was to determinate properties of CuCrZr alloy under cycling loading and model of W-CuCrZr.

#### Summary

Previous investigations based on determination of properties of W-Cu composites showed that by change of microstructure one can design properties of composites. The properties do not only depend on volume fraction of components but also upon their shape and arrangement. In order to simulate W-CuCrZr composites, the properties of CuCrZr alloy under monotonic and cyclic loading have been determined in range of temperatures from 20 to 550°C. Obtained mechanical data have been evaluated and parameters of isotropic-kineamtic hardening model have been determined. The parameters are presented in table 1.

	CuCrZr	W	CuCrZr_W 14%	CuCrZr_W 28%	CuCrZr_W 44 %
Specific Heat @ 20 °C [J/mm <sup>3</sup> -K]	388	129	351.74	315.48	274.04
Specific Heat @ 700 °C [J/mm <sup>3</sup> -K]	473	150	427.78	382.56	330.88
Density @ 700 °C [kg/mm <sup>3</sup> ]	8.92E-06	1.93E-05	1.04E-05	1.18E-05	1.35E-05
Density @ 700 °C [kg/mm <sup>3</sup> ]	8.58E-06	1.91E-05	1.01E-05	1.15E-05	1.32E-05
Conductivity @ 20 °C [W/mm-K]	0.318	0.175	0.297	0.278	0.255
Conductivity @ 700 °C [W/mm-K]	0.356	0.122	0.32324	0.290	0.253
E @ 20 °C [MPa]	114500	398000	125160	150679	175297
E @ 550 °C [MPa]	97000	383000	105450	131683	157160
Exp axial [1/K]	1.8E-5	1.529E-05	1.53E-5	1.258-05	1.08E-05
Exp transverse [1/K]	1.8E-5	1.59E-05	1.641E-05	1.48E-05	1.34E-05

In the numerical investigation computer generated random microstructures were used. The binary images have been translated into Abaqus pre-processor. For further numerical investigations only one type of composites structure was taken into consideration with ellipsoidal W particles of aspect ratio 3:1. This type of composites showed best alteration of thermal expansion coefficients through thickness and along longer diameter of tungsten inclusions. This feature provides better reduction of stress concentration at W-CuCrZr interface. Typical structures used for calculation are presented in Figure 2.

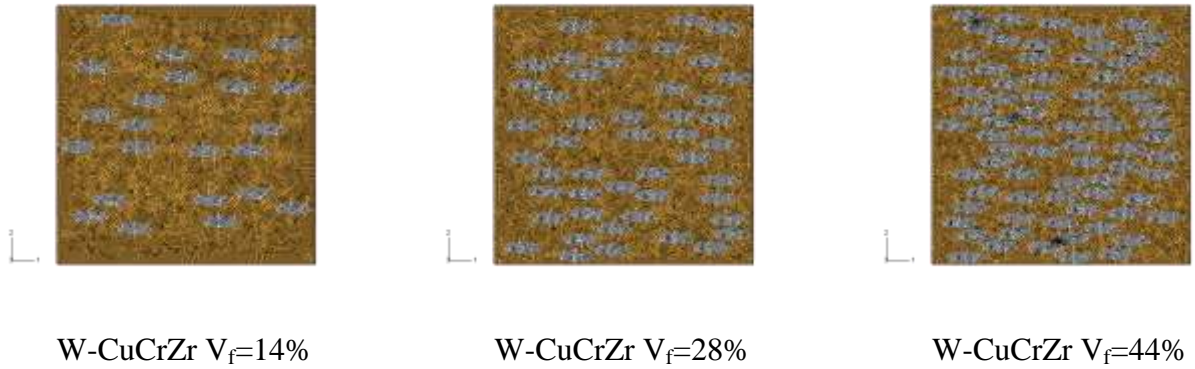


**Figure 1** Meshed structures of composites of different volume fraction of tungsten

From variety of structures three composites was chosen of tungsten volume fraction respectively 14%, 28% and 44%. Using these composites structures stress-strain behaviours at room and elevated temperatures have been calculated as well as anisotropy of CTEs. Other properties like specific heat, density was calculated employing simple rule of mixture, however conductivity was calculated using Eshelby formulation. Obtained mechanical properties of studied composite structures allowed to investigate influence of FGC on stress magnitude and stain magnitude in PFC. For the numerical analysis there was taken flat tile mock-up divertor component [1]. The calculations were carried out for three high heat flux heating and subsequent cooling cycles.

The properties of micromechanical composite models were homogenized and introduced as three layer interlayer between plasma facing material (tungsten) and heat sink (CuCrZr).

The plasma facing component have been loaded by impulse of plasma of power density  $15 \text{ MW/m}^2$  and neutrons that were simulated as internal generated heat in the entire structure respectively to the chemical composition. The PFC structure was cooled by water of temperature  $250^\circ\text{C}$  under pressure of  $15.5 \text{ MPa}$ . The schematic representation of boundary conditions is shown in Figure 2.

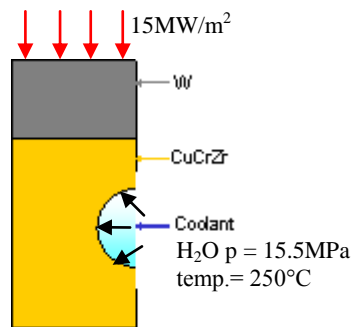


**Figure 2** Example of binary structure and FEM model of W-Cu composite

The temperature distribution did not differed significantly to those obtained in case of similar structure with W-Cu intrer layer. Thermal analysis and obtained temperature distribution have been employed into stress-strain analysis. PFC structure was numerically heated up to  $700^\circ\text{C}$  (brazing temperature of W-(W-CuCrZr)-CuCrZr interlayer, the component was cooled down to  $250^\circ\text{C}$  followed by three pulse plasma heating.

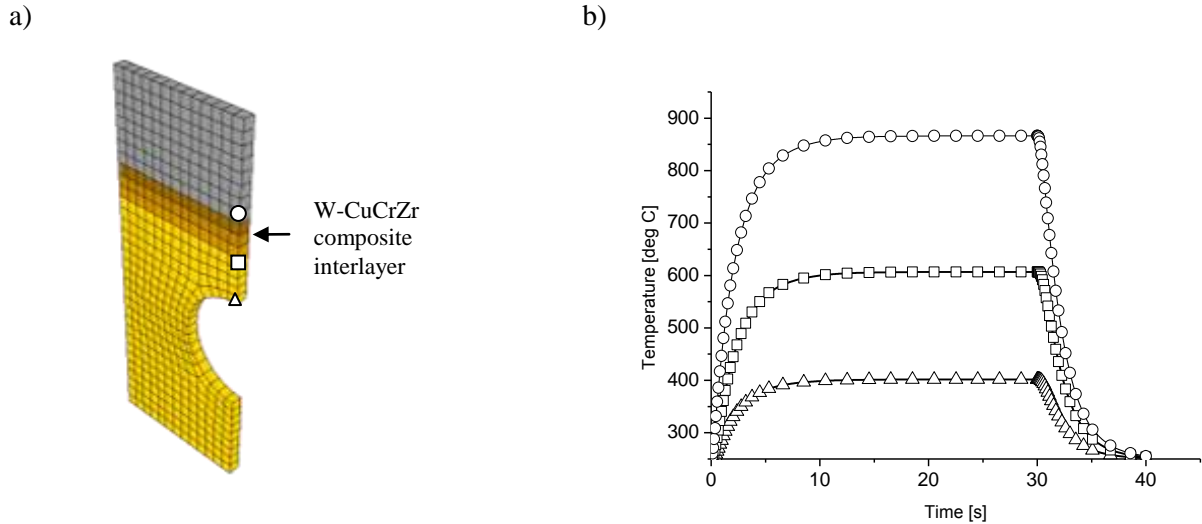


**Figure 3** a) PFC with W-CuCrZr intralayer, b) temperature distribution during plasma pulse

Tungsten PFM reveals strong stress at the interface related to higher yield of the W-CuCrZr FGC interlayer then investigated before W-Cu composite interlayer. There is also observed plastic flow in tungsten due to high temperature, however the plastic flow in not significant and tends to stabilization after initial cycles.

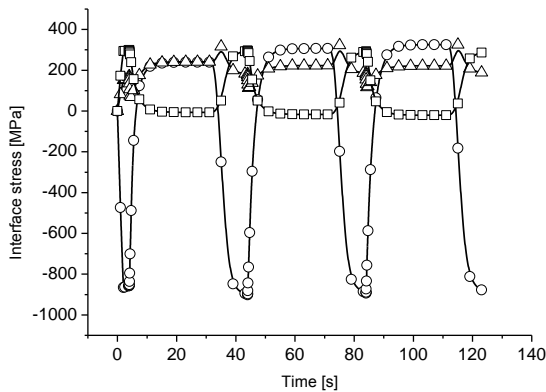


**Figure 4** Stress distribution at interface in tungsten, CuCrZr and at CuCrZr tube

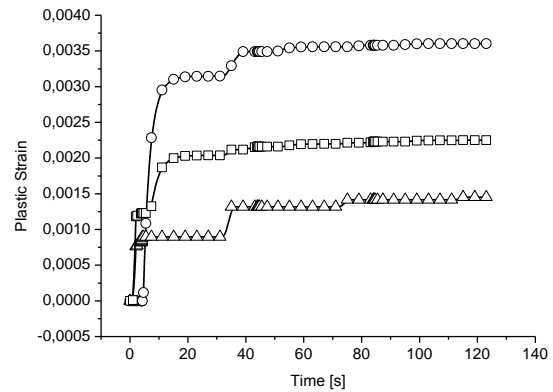


**Figure 5** Equivalent plastic strain in W PFM and CuCrZr HS

### Conclusions

- Once more incorporation of the FGC (W-CuCrZr) minimize plastic deformation at the interface which may prevent delamination and failure.
- The temperature distribution during plasma pulse heating almost do not depend upon the composite matrix be it Cu or CuCrZr
- Even if CuCrZr change its plastic resistance due to temperature and internal precipitation processes, the results for W-Cu composites showed that FGC interlayer would prevent and accommodate high interface mismatch

### Collaboration

Association EURATOM – IPP, Garching, Germany